VLSI Devices
Lecture 24

Sung-Min Hong (smhong@gist.ac.kr)
Semiconductor Device Simulation Laboratory
Department of Electrical Engineering and Computer Science
Gwangju Institute of Science and Technology (GIST)

Coverage

- Two YouTube lectures reserved for advanced topics
  - L14: ~~Substrate bias~~, ~~channel mobility~~
  - L15: ~~3.2.1~~
  - L16: ~~3.2.1 (Continued)~~
  - L17: ~~Velocity saturation (3.2.2)~~
  - L18: ~~Channel length modulation and so on (3.2.3, 3.2.4, 3.2.5)~~
  - L19: ~~MOSFET scaling~~
  - L20: ~~MOSFET scaling (Continued)~~
  - L21: Quantum effect (4.2.4)
  - L22: Double-gate MOSFETs (10.3)
  - L23: FinFETs
  - L24: CFETs

FinFET

- FinFET
  - Following its shape
  - Initially proposed as a SOI FinFET
  - Later, a bulk FinFET

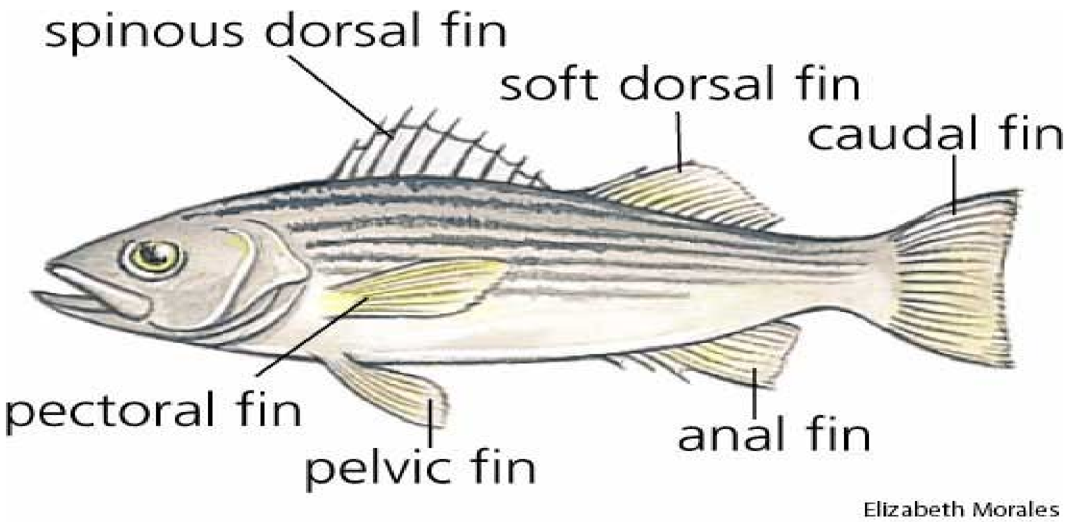

Fins (Google images)

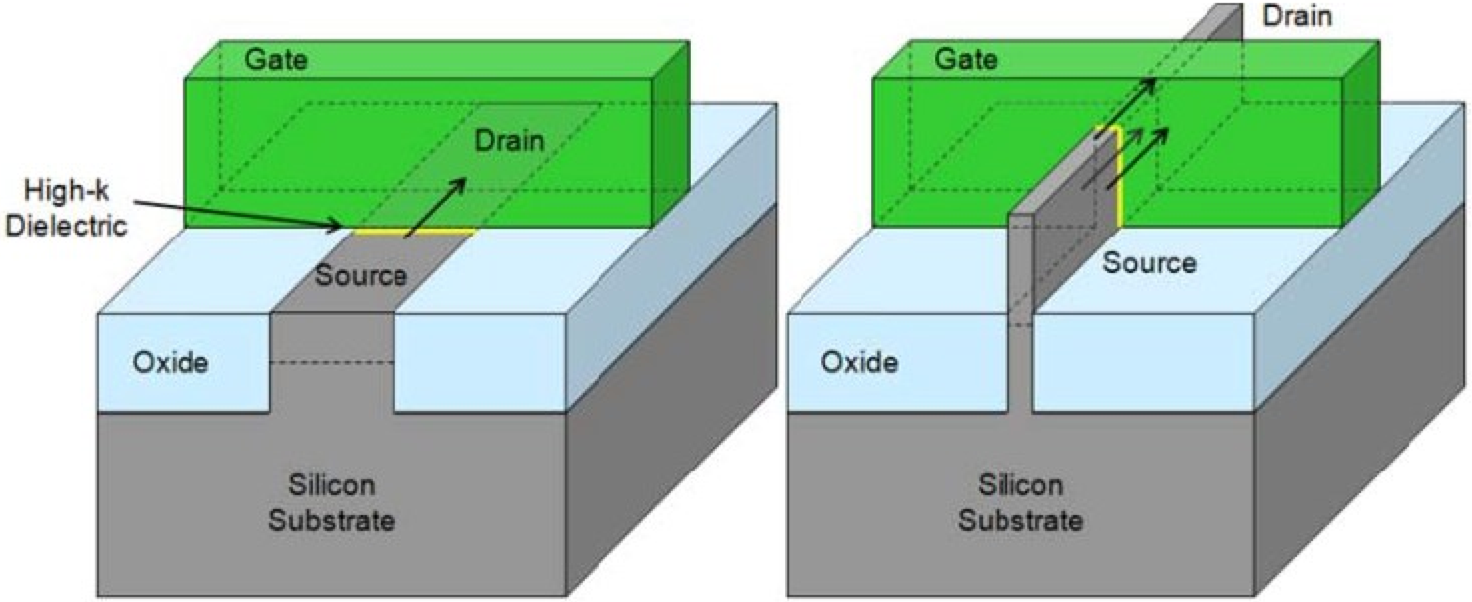

Planar transistor structure (left) and FinFET structure (right)

SEM image

- FinFET
  - Improved electrostatic control of the channel region

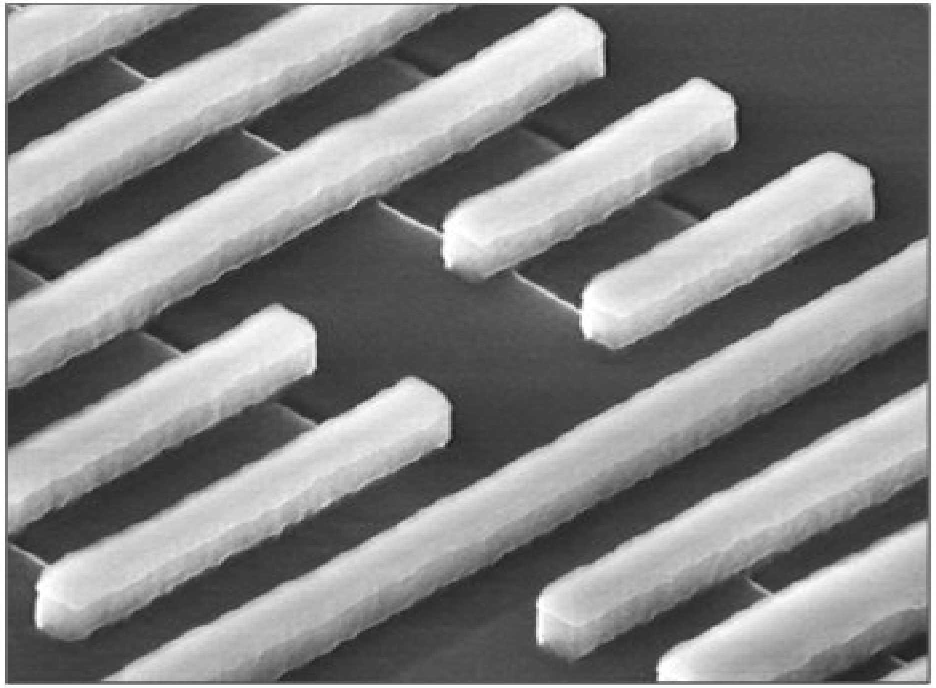

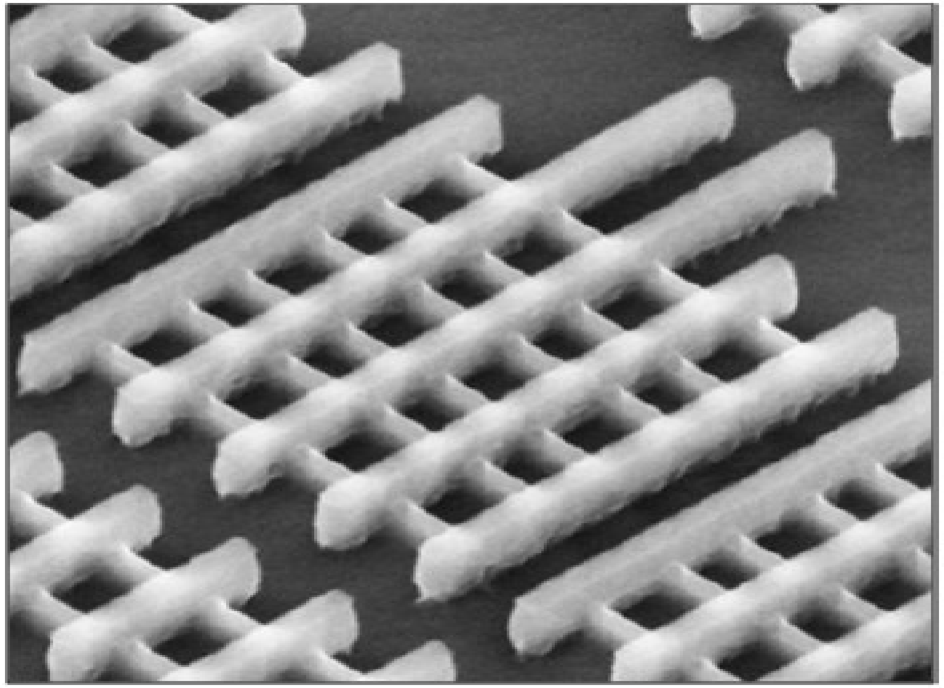

32nm planar transistors (left) and 22nm FinFETs (right)

Performance

- Steeper sub-threshold slope
  - × 10 off-state leakage reduction

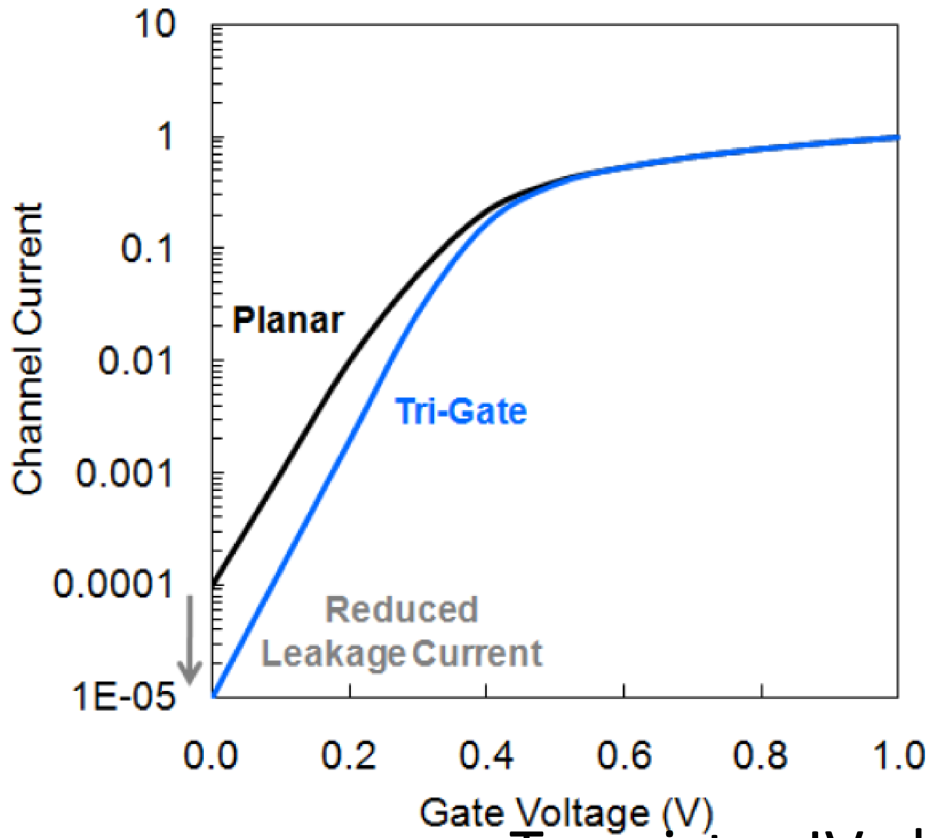

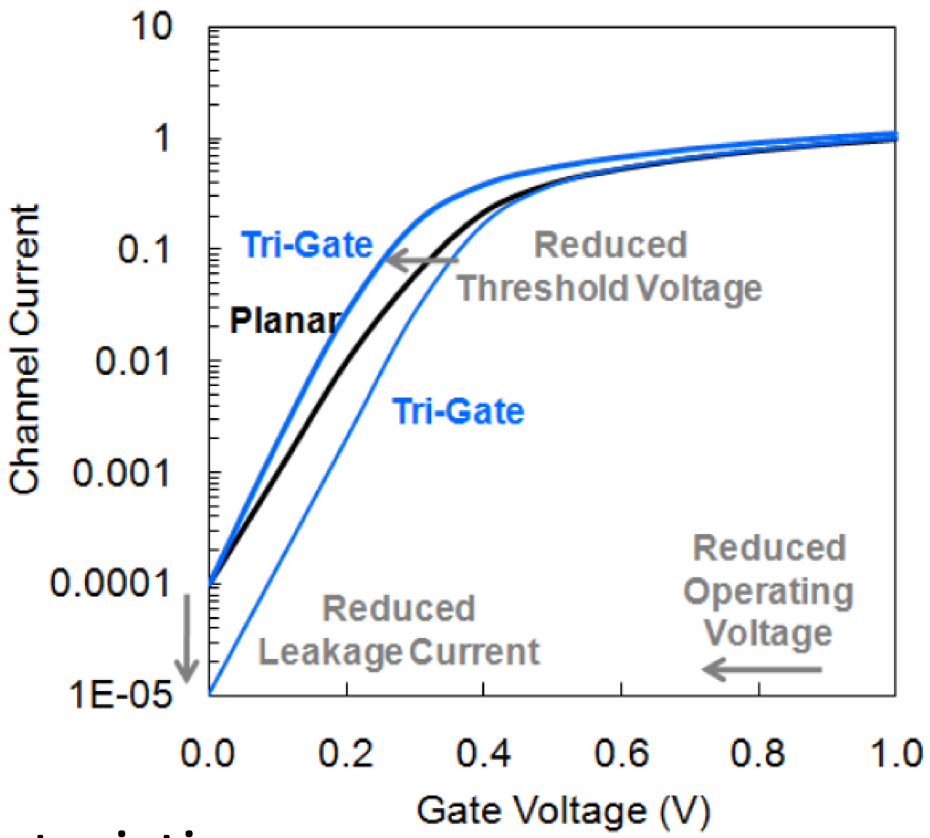

Transistor IV characteristics

Quantum effect

- Potential well formed by
  - The oxide barrier
  - The silicon conduction band
- Subbands
  - Quantized levels
  - Solutions of the Schrödinger equation
- Nearly zero n at the interface

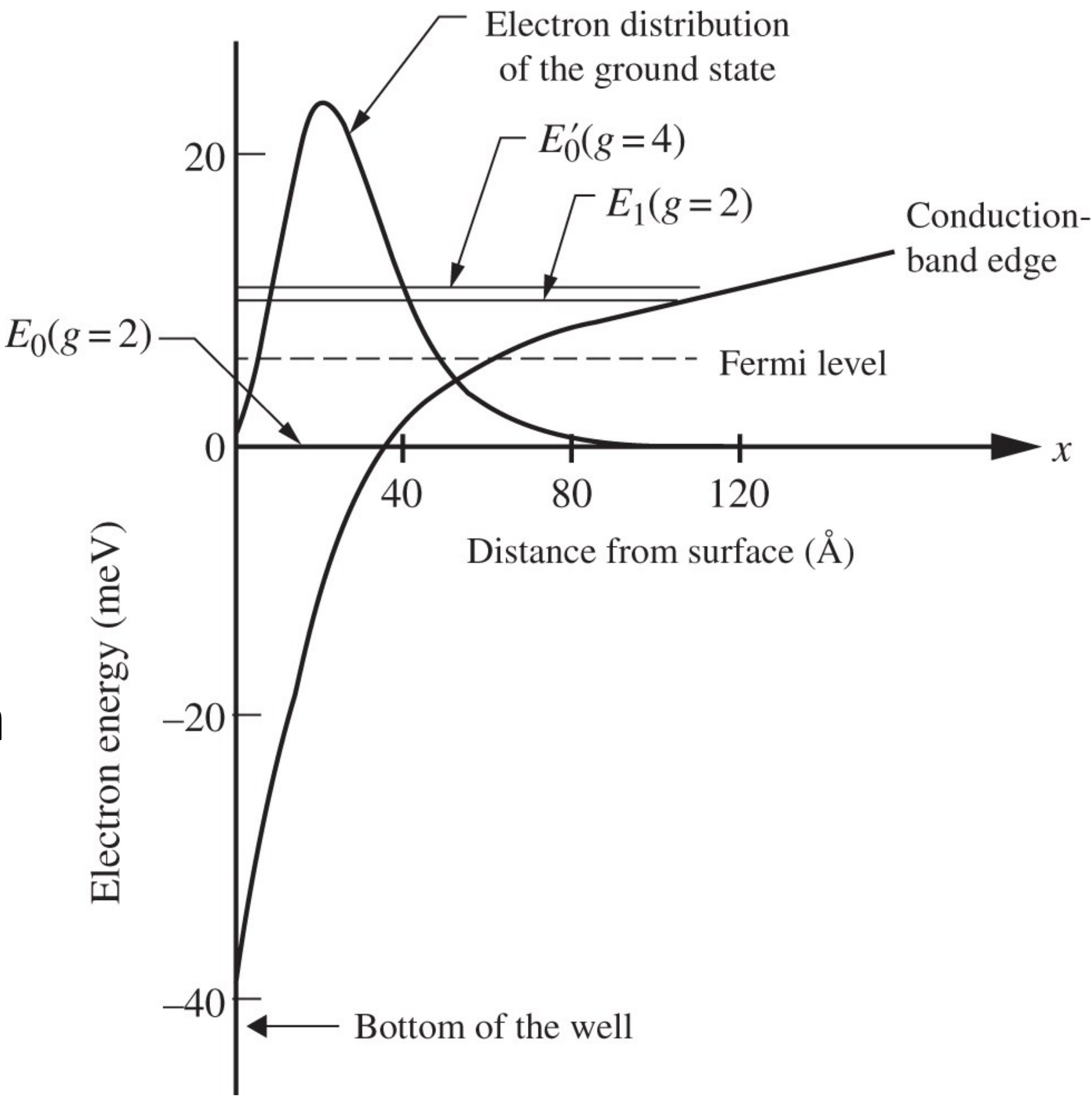

Energy levels of inversion-layer electrons (Taur, Fig. 4.18)

Electron profile

- Classical vs. quantum-mechanical
  - Maximum n at the interface
- Quantum mechanical effects
  - At high fields, V_t becomes higher.
  - Effective gate oxide thickness is larger.

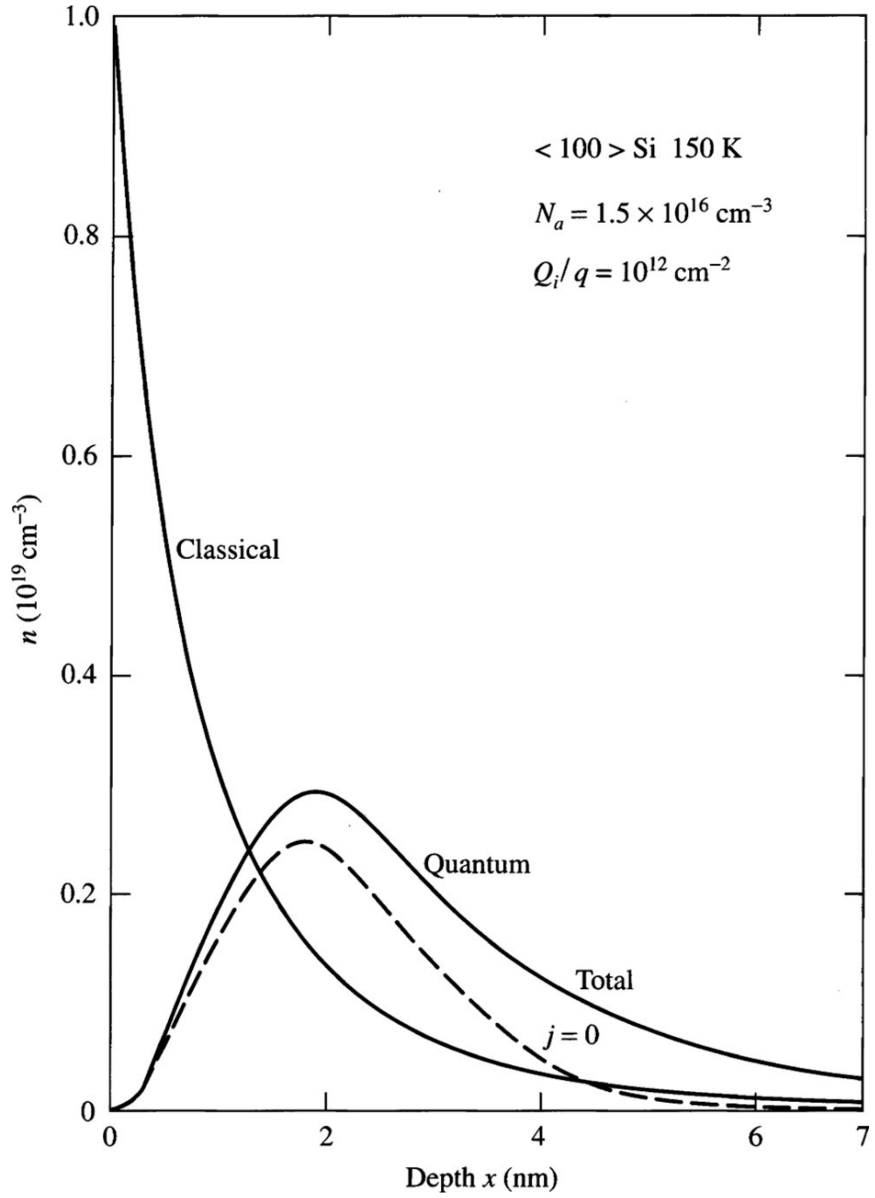

Classical and quantum-mechanical electron density (Taur, Fig. 4.19)

Poisson-Schrödinger solver

- General way to calculate the subband structure
  - It requires numerical analysis…
  - Interested? Watch my YouTube videos. (They are recorded in Korean.)

Triangular potential approximation

- Parabolic potential profile
  - However, it is further approximated as a linear potential. ➔ Triangular potential well
  - Then, the Schrödinger equation reads

$$\left[-\frac{\hbar^2}{2m_{xx}}\frac{d^2}{dx^2}+q\mathcal{E}_s x\right]\psi(x)=E\psi(x)$$

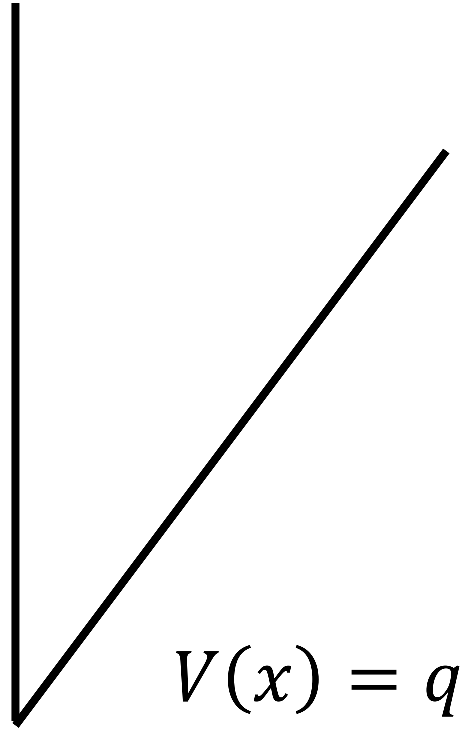

$V(x)=q\mathcal{E}_s x$

Its solution

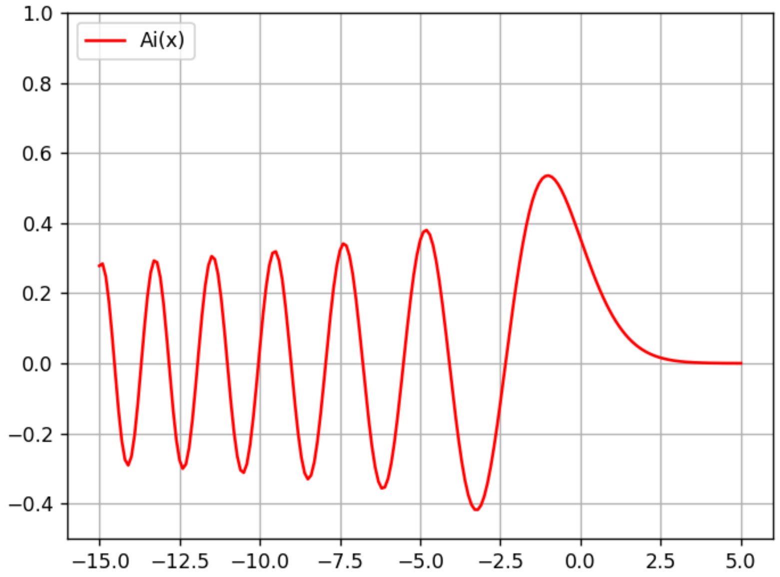

- Airy function

$$Ai(x) = \frac{1}{\pi}\int_0^\infty \cos\left(\frac{t^3}{3} + xt\right) dt$$

  - Its seond derivative is

$$\frac{d^2}{dx^2}Ai(x) = -\frac{1}{\pi}\int_0^\infty t^2 \cos\left(\frac{t^3}{3} + xt\right) dt$$

  - Note that $\frac{d}{dt}\sin\left(\frac{t^3}{3} + xt\right) = (t^2 + x)\cos\left(\frac{t^3}{3} + xt\right)$.
  - Therefore,

$$-xAi(x) + \frac{d^2}{dx^2}Ai(x) = -\frac{1}{\pi}\int_0^\infty \frac{d}{dt}\sin\left(\frac{t^3}{3} + xt\right) dt = 0$$

Simple manipulation

$$\frac{2m_{xx}}{\hbar^2}q\mathcal{E}_s$$

- The Schrödinger equation is written as

$$\left[\frac{d^2}{dx^2}-\frac{2m_{xx}}{\hbar^2}(q\mathcal{E}_s x-E)\right]\psi=\left[\frac{d^2}{dx^2}-\alpha^3\left(x-\frac{1}{q\mathcal{E}_s}E\right)\right]\psi=0$$

  - With a new variable, $\xi=\alpha\left(x-\frac{1}{q\mathcal{E}_s}E\right)$, it becomes

$$\left[\frac{d^2}{d\xi^2}-\xi\right]\psi=0$$

  - The solution is $\psi(x)\sim Ai(\xi)=Ai\left(\alpha\left(x-\frac{1}{q\mathcal{E}_s}E\right)\right)$.
  - At $x=0$, the wavefunction must vanish:

$$-\alpha\frac{1}{q\mathcal{E}_s}E_j=a_j$$

Zeros of the Airy function

$a_0\approx-2.3381$

$a_1\approx-4.0879$

Eigenenergy

- Zeros are well approximated as $a_j \approx -\left[\frac{3\pi}{2}\left(j+\frac{3}{4}\right)\right]^{2/3}$.
  - Then, the eigenenergy becomes

$$E_j = \frac{q\mathcal{E}_s}{\alpha}\left[\frac{3\pi}{2}\left(j+\frac{3}{4}\right)\right]^{2/3} = \left[\frac{3hq\mathcal{E}_s}{4\sqrt{2m_{xx}}}\left(j+\frac{3}{4}\right)\right]^{2/3}$$

Taur, Eq. (4.46)

  - There are two different m_{xx} values: $0.91m_0$ (degeneracy of 2, g=2) and $0.19m_0$ (degeneracy of 4 , g'=4)

Total inversion charge per unit area

- For a subband,
  - The number of electrosn per unit area

$$n = \frac{4\pi k_B T}{h^2} g\sqrt{m_y m_z} \ln\left[1 + \exp\frac{E_f - E_{min}}{k_B T}\right]$$

Taur, Eq. (A12.5)

  - Summation over subbands

$$Q_i^{QM} = -\frac{4\pi q k_B T}{h^2}\left(g m_t \sum_j \ln\left(1 + \exp\frac{E_f - E_c' - E_j}{k_B T}\right) + g'\sqrt{m_l m_t}\sum_j \ln\left(1 + \exp\frac{E_f - E_c' - E_{j'}}{k_B T}\right)\right)$$

Bottom of the conduction energy at the interface, $E_c' = E_c(\infty) - q\phi_s$

Taur, Eq. (4.49)

Subthreshold region

- In this case,
  - It is well approximated as

$$Q_i^{QM} \approx -\frac{4\pi q k_B T}{h^2}\left(g m_t \sum_j \exp\frac{-E_j}{k_B T} + g'\sqrt{m_l m_t}\sum_j \exp\frac{-E_{j'}}{k_B T}\right)\exp\frac{E_f - E_c'}{k_B T}$$

  - Using $E_c' = E_c(\infty) - q\phi_s$,

$$Q_i^{QM} \approx -\frac{4\pi q k_B T n_i^2}{h^2 N_c N_a}\left(g m_t \sum_j \exp\frac{-E_j}{k_B T} + g'\sqrt{m_l m_t}\sum_j \exp\frac{-E_{j'}}{k_B T}\right)\exp\frac{q\phi_s}{k_B T}$$

  - (Note that $\exp\frac{E_f - E_c(\infty)}{k_B T} = \frac{n_i^2}{N_c N_a}$.)

Taur, Eq. (4.50)

Shift of threshold voltage

- Q_i^{QM} is smaller than its classical counterpart.
  - Additional band bending is required to achieve the same inversion charge per unit area
  - Example taken from our textbook:
  - When N_a is 3 X 10^{18} cm^{-3}, $\Delta\phi_s^{QM}$ (additional surface potential to match the classical density) is 0.13 V.

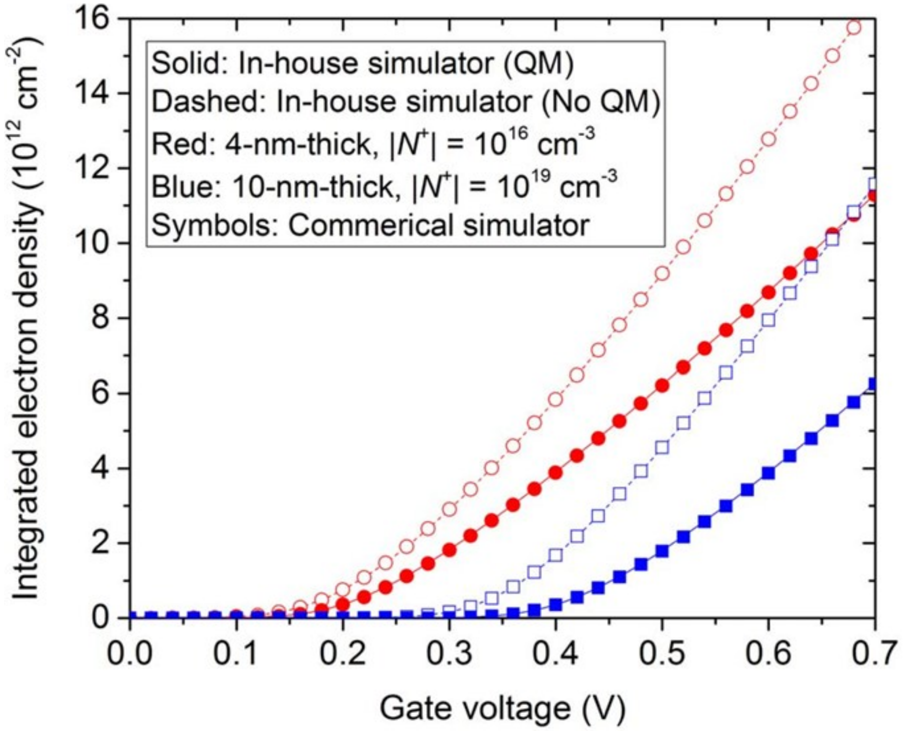

Q-V relations for double-gate MOS structures

Inversion-layer depth

- Average distance
  - It reduces at a high gate voltage.
  - However, QM value is larger than CL one.

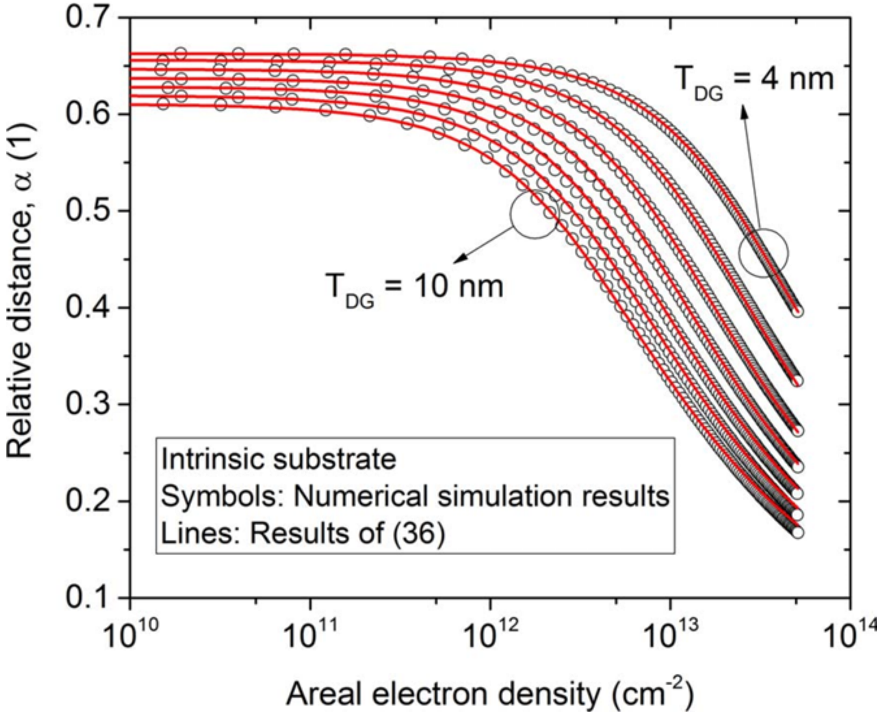

Average distance for double-gate MOS structures

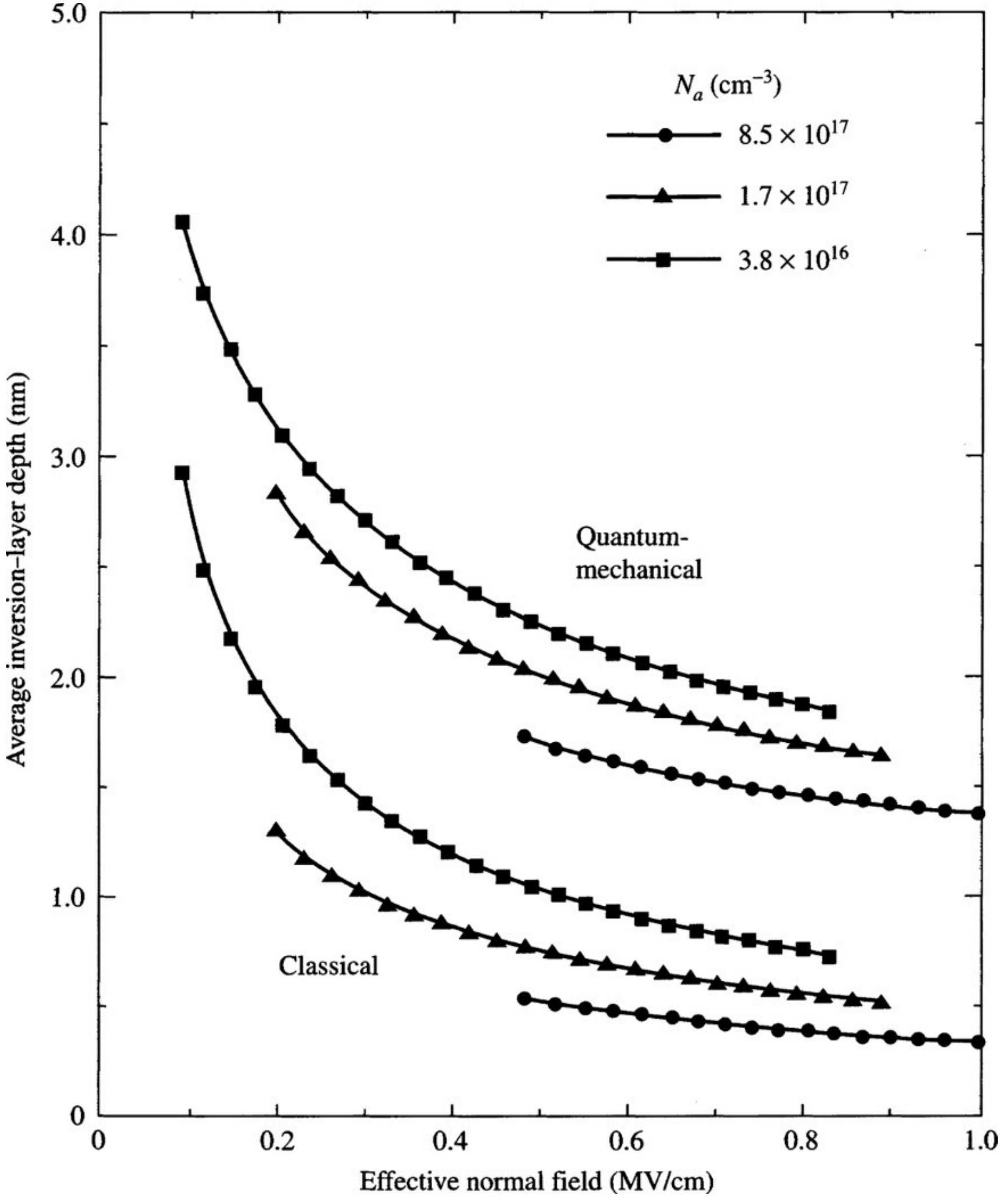

Inversion-layer depth (Taur, Fig. 4.21)

Thank you!